Stratified anisotropic structure at the top of Earth's inner core:a normal mode study

Jessica C.E. Irving, Arwen Deuss

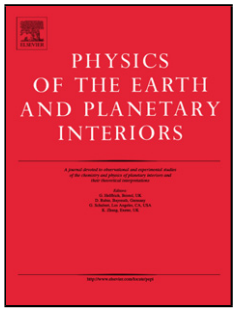

Title: Stratified anisotropic structure at the top of Earth's inner core:a normal mode study

Authors: Jessica C.E. Irving, Arwen Deuss

PII: S0031-9201(11)00055-0
DOI: doi:10.1016/j.pepi.2011.03.003
Reference: PEPI 5387

To appear in: *Physics of the Earth and Planetary Interiors*

Received date: 4-11-2009
Revised date: 31-1-2011
Accepted date: 9-3-2011

Please cite this article as: Irving, J.C.E., Deuss, A., Stratified anisotropic structure at the top of Earth's inner core:a normal mode study, *Physics of the Earth and Planetary Interiors* (2010), doi:10.1016/j.pepi.2011.03.003

We probe the isotropic layer at the top of Earth's inner core using normal modes.
Normal mode data are compatible with an isotropic layer of up to 250km thick.
Normal modes can therefore be reconciled with previous body wave studies.
We further show seismic data support the presence an S-wave isotropic layer.

Stratified anisotropic structure at the top of Earth's inner core: a normal mode study

Jessica C.E. Irving[a], Arwen Deuss[a]

[a] *Institute of Theoretical Geophysics & Bullard Laboratories, University of Cambridge, Madingley Road, Cambridge CB3 0EZ, UK. E-mail: jcei2@cam.ac.uk*

Abstract

Body wave studies support the presence of an isotropic layer at the top of the inner core. Recent normal mode models of inner core anisotropy do not contain such a layer, but instead have anisotropic structure extending to the inner core boundary. Here, we use full-coupling of normal mode oscillations sensitive to inner core structure in order to investigate the discrepancy between models of the inner core developed using these two different types of data. We impose an isotropic layer onto existing normal mode models of inner core anisotropy, and calculate frequencies, quality factors and synthetic seismograms for radial modes, PKIKP modes and PKJKP modes. Using full-coupling allows us to make the first simulations of the effect of an isotropic layer on radial modes. The presence of an uppermost isotropic layer has an effect on the frequencies and attenuation of normal modes. By calculating the misfit between data from four large earthquakes and synthetic seismograms created for models of the inner core with isotropic layers of varying thickness, we find that normal mode data are compatible with the presence of an isotropic layer of up to 250km thickness at the top of the inner core. Thus, normal modes can be reconciled with previous body wave studies. The influence of such a layer on PKJKP modes is the only way that S-wave isotropy at the top of the inner core can currently be studied; we show, for the first time, that seismological data support the presence an S-wave isotropic layer.

Keywords: Inner core, anisotropy, free oscillations.

1. Introduction

Earth's inner core has been probed using both normal mode and body wave data. Early studies using either of these techniques (Morelli et al., 1986; Woodhouse et al., 1986; Creager, 1992) proposed that the seismic velocity anisotropy in the inner core was both laterally invariant and depth-independent and that the axis of cylindrical anisotropy is aligned with Earth's rotation axis. More recent body wave studies have built up a picture of an inner core with a degree one 'hemispherical' structure (Tanaka & Hamaguchi, 1997; Creager, 1999; Oreshin & Vinnik, 2004) and a distinct innermost inner core where the anisotropy axis is at an angle of 45° to the anisotropy axis in the rest of the inner core (Ishii & Dziewonski, 2002; Cormier & Stroujkova, 2005; Cao & Romanowicz, 2007; Sun & Song, 2008).

Several authors (for example Shearer & Toy, 1991; Song & Helmberger, 1995; Yu & Wen, 2007) have suggested that the uppermost regions of the inner core, which have been most recently solidified (Jacobs, 1953), may not display any of the anisotropy characteristic of the intermediate regions of the inner core, but instead be isotropic. The presence of such an isotropic top layer could have strong implications for our understanding of the mechanisms which produce anisotropic texture in the inner core. In particular, those mechanisms which invoke the 'freezing-in' of the anisotropic fabric during the inner core's solidification (eg Karato, 1993b; Bergman, 1997) would require temporal variation of the conditions and processes at the inner core boundary in order to create an isotropic uppermost layer over the anisotropic deeper inner core.

Evidence for the isotropic nature of the uppermost inner core comes from a variety of body wave studies, which primarily use PKPdf, a P-wave which travels through the outer core, PKPbc and PKPab, which are P-waves which travel through the outer core but not the inner core, and PKiKP, a P-wave which is reflected off the inner core boundary. The primary techniques used to probe the isotropic layer are waveform modelling and the analysis of differential travel

times, which are the difference between the observed and predicted PKPbc-PKPdf or PKiKP-PKPdf travel times.

The first suggestion of the presence of an isotropic layer at the top of the inner core came from Shearer & Toy (1991) and Shearer (1994), who proposed that the top 50km of the inner core was isotropic using PKPbc-PKPdf differential travel time residuals and absolute travel time data. Song & Helmberger (1995) then used waveform modelling of the PKiKP and PKPdf phases to argue that to match the waveforms recorded for polar paths the top 60km of the inner core must be isotropic. It was also found that the anisotropy is weak in the region between 60km and 150km from the ICB. Further work (Song & Helmberger, 1998) using waveform modelling of the triplication caused by the velocity jump between an isotropic upper layer and an anisotropic lower layer lead these authors to suggest that the isotropic layer was 200km thick.

Both Creager (2000) and Garcia & Souriau (2000) suggested that the thickness of the isotropic layer was uneven, with a thinner (100-150km) isotropic layer on the western side and a thicker (400km) isotropic layer on the eastern side. Subsequently, Isse & Nakanishi (2002) and Niu & Wen (2002) have suggested that the isotropic layer in the eastern hemisphere is 190-200km thick, using both PKPdf-PKiKP and PKPbc-PKPdf differential travel times. Ouzounis & Creager (2001) suggest that the western hemisphere has a 50-150km thick isotropic layer. Rost & Garnero (2004) used two different seismic phases, PKKP and P′P′, (which travel through the core twice, and are internally reflected at either the core-mantle boundary or the surface of the Earth) in contrast to earlier studies. Phase-weighted stacks of array data which sample both the eastern and western hemispheres of the inner core suggest that there may be anisotropy (up to 7%) or strong heterogeneities in the top 100km of the inner core, in contrast to earlier studies. Yu & Wen (2007) used PKPdf-PKiKP differential travel times and amplitude ratios to investigate the structure of the inner core under Africa where the boundary between the eastern and western hemisphere of the inner core is located. They found no isotropic layer under eastern Africa, whilst the uppermost isotropic layer under western Africa is up to 50km thick.

Below this isotropic layer there is a velocity jump for the polar paths of about 2%, suggesting that the inner core anisotropy is still lower than that found at greater depths by other authors. Whilst there is a growing consensus that the top of the inner core may be isotropic, the details of this layer, in particular its thickness and geographical variation, are still a matter of uncertainty.

Here we investigate the compatibility of these body wave results with normal mode data. Symmetry considerations require that normal mode oscillations of the Earth are not sensitive to the velocity structure at the centre of the Earth, and in general their sensitivity is larger at the inner core boundary (ICB) than deeper in the inner core. Inner core anisotropy splits the spectra of normal mode oscillations, which led early normal-mode studies to assume that the anisotropy must be concentrated in the upper part of the inner core.

The earliest normal mode model of inner core anisotropy (Woodhouse et al., 1986) is a depth independent model, so that the presence of an isotropic layer at the top of the inner core was not possible. The strongest anisotropy in the model produced by Tromp (1993) is at the ICB. An inversion using both body-wave and normal mode data was carried out by Durek & Romanowicz (1999); the body wave data used were PKPab-PKPdf differential travel times, which are not particularly sensitive to to the distribution of anisotropy at the top of the inner core. They found that the fit of the model to the data was degraded if an isotropic uppermost layer of thickness greater than 200km was introduced into the model. Beghein & Trampert (2003) developed an inner core anisotropy model by inverting splitting functions. Like the models of Durek & Romanowicz (1999) and Woodhouse et al. (1986) this model contains anisotropic structure at both the ICB and centre of the inner core; none of these models contains isotropic structure at the top of the inner core.

We use these four normal mode models of inner core anisotropy - the B&T model (Beghein & Trampert, 2003), the D&R model (Durek & Romanowicz, 1999), the Tr model (Tromp, 1993) and the W,G&L model (Woodhouse et al., 1986) - to examine the apparent discrepancy between the anisotropic structure at the top of the inner core observed using normal modes and the isotropic

structure found by previous body wave studies. All of these models have been made using the self-coupling (SC) approximation, which we have shown (Irving et al., 2008) to be inaccurate when inner core anisotropy is considered. The use of full-coupling (FC) of normal modes is computationally more intensive than using SC, but provides a more realistic description of the oscillations of the Earth, and may permit the reconciliation of body wave and normal mode data.

2. Methodology

Normal modes are oscillations of the whole earth. Each oscillation has a characteristic frequency (ω) and quality factor (Q). The spheroidal normal modes can be described using the notation ${}_nS_l$, where n is the overtone number and l the angular order of the mode. n corresponds to the number of nodes in the eigenfunction of a radial mode as a function of depth. l corresponds to the number of nodal lines an eigenfunction has on the surface of the Earth. The frequencies of these modes can then be written ${}_n\omega_l$. For a spherically symmetric, non-rotating Earth model, each mode consists of a $(2l+1)$-fold degenerate multiplet, whose singlets all have the same frequency. Aspects of the Earth which deviate from the spherically symmetric, non-rotating Earth model, such as the elliptical shape of the Earth, or lateral heterogeneity within it, remove the degeneracy of the normal modes so that each mode multiplet is split into a set of $(2l+1)$ singlets with different frequencies. These singlets are labelled by their azimuthal order, m, where m takes integer values $-l \leq m \leq l$.

Existing models of inner core anisotropy have been developed using the self-coupling (SC) approximation, which assumes that lateral heterogeneities in the earth, for example anisotropy or lateral velocity structure, does not cause coupling, or interactions, between normal modes. When using SC it is therefore possible to treat each mode as isolated. In addition to splitting of individual modes, cross-coupling, or resonance between between different modes, also occurs, which again changes the frequencies of the singlets. In Irving et al. (2008)

we showed that the effects of full-coupling (FC), where large groups of modes are allowed to couple, are significant when inner core anisotropy is included in the calculations, so that using SC is unsatisfactory.

[Figure 1 about here.]

The inner core sensitive modes discussed in this study can be divided into three types: PKIKP, PKJKP and radial modes. PKIKP modes have sensitivity to both changes in v_p and v_s in the inner core whilst PKJKP modes are sensitive only to inner core v_s. Radial modes have eigenfunctions that are spherically symmetric, and are sensitive to both v_p and v_s in the inner core; they are a special type of PKIKP mode and tend to decay much more slowly than PKIKP modes so that they can be observed over longer time windows. The sensitivity kernels of two radial modes ${}_2S_0$ and ${}_5S_0$, two PKJKP modes ${}_9S_4$ and ${}_{11}S_5$ and two PKIKP modes ${}_{13}S_1$ and ${}_{13}S_2$, are shown in Figure 1. Some of the modes are most sensitive to inner core structure near the ICB (for example ${}_{11}S_5$), whilst others, like ${}_5S_0$, are more sensitive to velocity and density perturbations deeper in the inner core.

Here, we focus on those modes which are sensitive to inner core structure and have a frequency below 7mHz. The frequencies and quality factors of 97 inner core sensitive modes were calculated for mantle and inner core structure with the modes permitted to either fully-couple (as described in Irving et al., 2008) or to self-couple. We identified 19 'target' modes, which strongly react to the inclusion of an isotropic layer at the top of the inner core and studied these modes in detail. As various authors (including Dahlen, 1969; Park, 1986; Resovsky & Ritzwoller, 1995; Deuss & Woodhouse, 2001) have shown that normal modes can couple through mantle structure, it was important to include in each calculation a band of mantle and crust sensitive normal modes which may couple with the core mode of interest (the target mode). As normal modes become more tightly packed with increasing frequency, the width of the band of mantle modes included in each calculation decreases as the frequency of the target mode increases. The bands of modes coupled, together with the frequency

of each target mode, are shown in Table 1. Each target mode is also coupled to all the other inner core sensitive modes. By investigating the sensitivity to 1-D changes in inner core v_s and v_p (the method described by Deuss, 2008), each of the 19 'target' normal modes studied was characterised as a radial, PKIKP (sensitive to change in both v_s and v_p in the inner core) or PKJKP mode (sensitive to v_s but not v_p in the inner core).

[Table 1 about here.]

All calculations also include the effects of coupling through ellipticity, rotation and mantle structure. Shear wave model S20RTS (Ritsema et al., 1999) was used to describe lateral variations in mantle velocity and density. The shear wave velocity perturbations were scaled to obtain compressional velocity, v_p, and density, ρ, with scaling of the form $\delta v_p/v_p = 0.5\delta v_s/v_s$ (Li et al., 1991) and $\delta\rho/\rho = 0.3\delta v_s/v_s$ (Karato, 1993a). PREM (Dziewonski & Anderson, 1981) was used to provide the 1-D velocity and density structure of the Earth. Synthetic data were compared with data from four earthquakes: the 1994 June 9$^{\text{th}}$ Bolivia earthquake (060994A), 1994 October 4$^{\text{th}}$ Kuril earthquake (100494B), 1995 July 30$^{\text{th}}$ Chile earthquake (073095A) and 2004 December 26$^{\text{th}}$ Sumatra earthquake (122604A). The location and magnitude of each of these events are shown in Table 2. We use the CMT catalogue (`www.globalcmt.org`). The Sumatra event is corrected for its long source duration following Park et al. (2005). We tested the Tsai et al. (2005) model, and found that at normal mode frequencies below 7mHz the difference is mainly in increasing the amplitude as compared to the CMT mechanism, which is comparable to the effect of the source duration correction we use.

The data from the three earliest of these events were used by Durek & Romanowicz (1999) and the Bolivia and Kuril events were part of the splitting function dataset used by Beghein & Trampert (2003) in their inversion for an inner core anisotropy model. The vertical component of the synthetic and real seismograms are cosine tapered and Fourier transformed to the frequency domain before both the amplitude and phase information are studied.

[Table 2 about here.]

The presence of an isotropic layer, of thickness ranging from 0km to 1150km was imposed upon the anisotropy models in each calculation. The different thickness of the isotropic layer used were separated by 25km intervals between 0km and 600km, and by 50km intervals between 600km and 1150km.

To determine how well synthetic seismograms created for a specific inner core anisotropy model fit the data collected for a particular earthquake, the complex misfit between the data and each synthetic seismogram was calculated:

$$\text{misfit} = \frac{1}{N}\sum^{N}\frac{\sum_{i=1}^{n}|z_{data,i}-z_{synth,i}|^2}{\sum_{i=1}^{n}||z_{data,i}|+|z_{synth,i}||^2} \quad (1)$$

where there are N spectral segments which each contain n data points in frequency space and z is the complex spectrum and includes both phase and amplitude information.

3. Frequency and Q response to an isotropic top layer

We first investigate the effect of the inclusion of an isotropic layer on the frequency and attenuation of several different normal modes.

3.1. PKJKP mode ${}_{11}S_5$

${}_{11}S_5$ is a PKJKP mode, sensitive only to shear wave velocity in the inner core. It has been used in the inversions which created all four of the anisotropy models we use here. Creager (2000) shows the self-coupling sensitivity kernel of ${}_{11}S_5$ (Figure 1(d)) and claims that the body-wave observations of an isotropic layer disagree with normal mode results. The sensitivity kernel of ${}_{11}S_5$ suggests that the mode is only affected by the structure at the top of the inner core. However, ${}_{11}S_5$ observations cannot be accounted for without invoking inner core anisotropy, which leads to the conclusion in Creager (2000) that normal mode results demand there must be anisotropy at the top of the inner core.

Figure 2 shows the response of ${}_{11}S_5$ to the introduction of an isotropic layer. It is clear that the frequencies and quality factors of the singlets change even

when the sensitivity of the mode appears to be negligible. For example, the quality factor (Q) of the lowest frequency singlets reach a minimum when the isotropic layer is 300km thick when using both the B&T (Figure 2 (a)) and Tr (Figure 2 (c)) models and do not reach their limiting value until the isotropic layer is 600km thick.

[Figure 2 about here.]

The behaviour of ${}_{11}S_5$ shows that the self-coupling isotropic sensitivity kernels may no longer be accurate when considering an anisotropic inner core using full-coupling. The SC sensitivity kernels do not reflect the true sensitivity of this mode because FC will cause ${}_{11}S_5$ to couple with other modes, changing the eigenfunction and therefore the sensitivity kernel of ${}_{11}S_5$. Furthermore, the sensitivity of modes to the inner core may only be a fraction of that to mantle structure, but anisotropic structures in the inner core can still cause changes in the frequency and Q of those modes.

The use of modes such as ${}_{11}S_5$ also allows us to model the effects of a layer in which the shear wave velocity is isotropic. Observations of shear waves in the inner core are limited (Deuss et al., 2000; Cao et al., 2005; Cao & Romanowicz, 2009) and only one attempt to observe shear-wave anisotropy using PKJKP has ever been made (Wookey & Helffrich, 2008). Furthermore, PKJKP is a major-arc phase, which is refracted towards the centre of the Earth at the ICB due to the low shear velocity in the inner core. This means that, unlike compressional body waves, there are no PKJKP body waves which sample only the uppermost inner core. The use of PKJKP modes will be essential in understanding whether shear waves at the top of the inner core travel through an isotropic or anisotropic fabric.

3.2. Radial mode ${}_2S_0$

If ${}_2S_0$, which has the sensitivity kernels shown in Figure 1(a), was only permitted to self-couple there would be no change to the frequency or Q of the

mode, as self-coupling rules do not permit radial modes to respond to 3-D structure. The use of full-coupling allows ${}_2S_0$ to interact with other modes through the 3-D anisotropic structure present in the inner core (as well as through the heterogeneous structure of the rest of the Earth). Figure 3 shows how the frequency and Q of mode ${}_2S_0$ vary with the inclusion of an isotropic top layer when FC is used. The changes are non-linear, and depend on the coupling interactions cause by the different anisotropy models. The scale of the frequency changes varied strongly between the four models - the frequency of ${}_2S_0$ ranges between 2.5061mHz and 2.5105mHz when the W,G&L model is used (Figure 3 (d)), but between 2.5098mHz and 2.5102mHz only when the Tr model is used (Figure 3 (c)).

[Figure 3 about here.]

[Table 3 about here.]

The frequency and Q of ${}_2S_0$ have been measured by several authors, as shown in Table 3. The earlier of the observed values have Q much higher than for those calculated for the four anisotropic models. This is because the calculations are based on PREM, which underestimates the Q for this mode when compared to those observations. The range over which the frequency of ${}_2S_0$ varies in the observations is comparable to the range over which it varies when an isotropic layer is imposed at the top of the inner core.

3.3. PKIKP mode ${}_{13}S_1$

PKIKP mode ${}_{13}S_1$ has been used in the construction of both the D&R and B&T inner core anisotropy models, as it responds strongly to anisotropic structure in the inner core; its sensitivity kernel is shown in Figure 1(e). The variations in the frequency and Q of the three singlets in ${}_{13}S_1$ are shown in Figure 4. The variations are again model dependent, and highly non-linear. When an isotropic layer is imposed on the top of an anisotropy model, both the frequency and quality factor (Q) of the mode change. The $m = 0$ singlet

reacts especially strongly to the imposition of an isotropic layer when the B&T model (Figure 4 (a)) is used. However, the changes when the isotropic layer is thin (0-200km) are small for all models, so that ${}_{13}S_1$ is less useful than ${}_2S_0$ at discriminating between different thin isotropic layers; instead ${}_{13}S_1$ will provide information about the anisotropy structure deeper in the inner core.

[Figure 4 about here.]

4. Observable changes in spectra

As we have shown in the previous section, the inclusion of an isotropic layer can have a dramatic effect on the frequency and Q of a mode. It is therefore expected that the shape and position of a mode in the frequency domain will vary as the isotropic layer is thickened. Synthetic seismograms were created for all of the modes shown in Table 1, for each model and the range of isotopic thicknesses described in Section 2. Here, we show the seismograms for three such modes, which are representative of the general influence of an isotropic layer at the top of the inner core.

4.1. Radial mode ${}_5S_0$

Whne the B&T model is used, the centre of the spectral peak of radial mode ${}_5S_0$ (Figure 5) decreases in frequency as an isotropic layer at the top of the inner core is thickened. The frequency calculated for this mode decreases from 4.8883mHz to 4.8870mHz as the layer thickness increases from 0 to 250km. The frequency of the spectral peak in the data for this station (which has been scaled in Figure 5, see caption for details), event and time window agrees best with an isotropic layer thickness of 25km. There is also a slight increase in the amplitude of the mode as the layer thickness increases, corresponding to an increase in Q; the amplitude of the data is twice that of all of the synthetic seismograms. The frequency and attenuation of this radial mode are unchanged by the presence of an isotropic top layer in the inner core when SC is used as radial modes are only sensitive to variations of 1-D structure in the self-coupling approximation.

[Figure 5 about here.]

The sensitivity kernels for ${}_5S_0$ are shown in Figure 1(b); observations of the frequency and Q for this mode are shown in Table 4. An isotropic layer thickness 0km best fits the frequency observed by Masters & Gilbert (1983), He & Tromp (1996) and Masters (2009) whilst an isotropic layer thickness of 225km best fits the prediction of Dratler et al. (1971).

[Table 4 about here.]

4.2. PKIKP mode ${}_{13}S_2$

Mode ${}_{13}S_2$, a PKIKP mode which has the sensitivity kernels shown in Figure 1(f), is identified by several authors (Deuss, 2008; Durek & Romanowicz, 1999) as an unusual mode. Deuss (2008) showed that two different inner core shear velocities are consistent with data collected for ${}_{13}S_2$. When inversions for its splitting function are performed, at least two different alternative solutions are possible: the splitting function found is dependent upon the starting model (Durek & Romanowicz, 1999). The difficulties in resolving the splitting function of this mode caused it to be excluded from the inversion which produced the B&T model.

[Figure 6 about here.]

Figure 6 shows the behaviour of ${}_{13}S_2$ as an isotropic layer is introduced at the top of the inner core for station ARU for the W,G&L model with FC. When there is no isotropic layer present (the thick red line in Figure 6), the mode is seen at station ARU as a widely split peak, with two singlets making up the lower peak and three singlets in the higher peak. As the thickness of the isotropic layer increases, the amplitudes of the two peaks become more disparate; the lower frequency peak decreases in amplitude and increases in frequency while the higher frequency peak decreases in frequency. Increasing layer thickness causes the two peaks to coalesce and merge into a single peak. Data for this station has one widely split peak with a maximum amplitude at 4.8447 mHz;

this station would best agree with an isotropic layer thickness of 375km if only the amplitude of the data was considered; it best agrees with an isotropic layer thickness of 1000km when both amplitude and phase of the data are taken into account.

4.3. PKJKP mode ${}_9S_4$

Figure 7 shows an example of the behaviour of ${}_9S_4$ as an isotropic layer is introduced at the top of the inner core for station ENH using the D&R model with FC. This mode is sensitive only to v_s in the inner core, and not to inner core v_p, as can be seen in its sensitivity kernel (Figure 1(c)). When there is no isotropic layer present (the thick red line in Figure 7), the frequency spectrum of this mode is seen at station ARU as a single peak which is broad due to the separation in frequency of the singlets. The introduction of an isotropic layer causes the mode to separate into two peaks, and as the layer thickness increases the relative amplitudes of the two peaks change. This trend reverses as the layer thickness increases further and as the thickness of the isotropic layer reaches 175km the two peaks re-combine into one peak. As the thickness of the isotropic layer continues to increase beyond 250km, this single peak undergoes only small changes in central frequency although the amplitude of the peak continues to vary. Data for this station and time window (shown as a black dashed line in Figure 7) has one peak, centred at 3.8772mHz; the amplitude of of the spectrum is best fitted by the presence of an 225km thick layer for this station, but when the phase of the data is also taken into account this spectrum is best fitted by the presence of a 700km thick isotropic layer when the D&R model is used.

4.4. Frequency spectrum

A portion of the frequency spectra for the Bolivia event (060994A) is shown in Figure 8. There are three prominent inner core sensitive modes present in this range, as well as 35 mantle or crust sensitive normal modes. By starting the time window thirty hours after the event, most of the mantle and crust

sensitive modes have decayed away; the inner core sensitive modes dominate the spectrum. Synthetic synthetic seismograms for the Tr model with no isotropic layer and a 225km thick isotropic top layer are also shown. Neither a 225km thick isotropic layer nor the absence of an isotropic layer fully replicates the split peak of PKIKP mode ${}_{11}S_1$, though the fit is better when there is no isotropic layer for this station when both phase and amplitude are considered.

[Figure 7 about here.]

The absence of an isotropic layer produces a split peak for PKJKP mode ${}_9S_3$ which is not seen in the data, a single peak is replicated by a 225km thick isotropic layer, all be it with too great an amplitude. The phase of ${}_9S_3$ is better matched when there is no isotropic layer although the amplitude is better fitted by the 225km isotropic layer. PKJKP mode ${}_9S_4$ has a split peak in the data but neither a 225km isotropic layer or the absence of an isotropic layer is capable of reproducing this effect.

From this spectral segment it can be seen that the incorporation of an isotropic layer into the Tr model improves the fit of some modes, but worsens the fit of others in this frequency range; there is no clear-cut preferred layer thickness for this station and event.

5. Searching for the isotropic layer

The misfit (Equation 1) between synthetic seismograms and data from the four events listed in Table 2 was calculated for both FC and SC spectra. For each event, time and frequency windows containing each one of 19 inner core sensitive modes were selected for up to 52 stations. Modes were characterised as PKIKP (sensitive to inner core v_p and v_s) or PKJKP (sensitive to inner core v_s only) or radial.

[Figure 8 about here.]

5.1. PKIKP modes

PKIKP modes permit an isotropic layer of up to 225km with all models using FC (Figure 9 (a)), but do not rule out the absence of an isotropic layer. Different PKIKP modes strongly favour different isotropic layer thicknesses for different models.

The depth range over which the modes respond to an isotropic layer varies widely. For example, the mode pair ${}_{11}S_2$ and ${}_{10}S_2$ exhibits sensitivity to inner core anisotropy even when the top 1100km of the inner core is isotropic.

5.2. PKJKP modes

The misfits for PKJKP modes (Figure 9(b)) show that, using FC, all four models fit the PKJKP data better when there is an isotropic top layer of between 0 and 300km thickness. The B&T model has two minima in misfit, for layers of 50km and 275km, the D&R model has a minimum at 225km, the Tr has two minima at 0km and 300km and the W,G&L has a minimum at 75km. The misfits when SC is used are, like those for the PKIKP modes, higher than the FC misfits.

The separation of the PKJKP modes from those modes which are sensitive to inner core v_p permits an analysis of the inner core S-wave anisotropy. A shear wave through the inner core has only been observed for a few events (Deuss et al., 2000; Cao et al., 2005; Wookey & Helffrich, 2008), and only when seismograms are stacked to enhance the signal-noise ratio. No inner core S-wave anisotropy has ever been observed in a single seismogram. The response of these PKJKP normal modes is therefore the best information we have about S-wave anisotropy. The PKJKP modes show that inner core anisotropy is not confined to P-waves, but also affects S-waves: when all of the PKJKP modes are considered together, the misfit for an anisotropic core is smaller than that for an isotropic inner core. Shear wave isotropy at the top of the inner core is supported by all four models; this result is the first time that shear wave isotropy at the top of the inner core has been observed.

5.3. Radial modes

Using FC, the misfits for radial modes (Figure 9 (c)) vary depending on the inner core anisotropy model used; radial modes were not used in any of the inversions which created the four anisotropy models used here. Overall, three of the four models have smallest misfits between the data and synthetics when there is no inner core anisotropy at all; this is because the models used were created using SC. Coupling rules (Luh, 1974) do not allow radial modes to be affected by inner core anisotropy when SC is used. The imposition of an isotropic layer has a much smaller effect on the radial modes when the Tr model is used than when the other three models are used. The sensitivity of these radial modes to anisotropic structure in the inner core emphasise the failings of SC when inner core anisotropy is considered.

5.4. Combining all modes

The best fitting isotropic layers for each model using FC and SC are shown in Figures 10 (a) and (b) respectively and Table 5. The error bounds quoted in Table 5 are the isotropic layer thicknesses for which the misfit is within 0.005 of its minimum value. The misfit is higher when the core is completely isotropic than when any of the anisotropy models is used. This finding confirms that inner core anisotropy fits normal mode data better than an isotropic model of the inner core. Using FC, three of the models (B&T, D&R and Tr) have two distinct minima, at 0km and 225-275km. The W,G&L model (which originally had no dependence of anisotropy on radius) has one minima, at 25km. However, as can be seen in Figure 10(a), the difference in misfit between a 100km isotropic layer and no isotropic layer is sufficiently small that the presence of a slightly thicker isotropic layer cannot be ruled out. Beyond an isotropic layer thickness of 300km, the misfit between data and synthetic seismograms increases for all the models.

[Figure 9 about here.]

[Table 5 about here.]

The misfit between the synthetic seismograms and the data is increased when SC is used instead of FC. The SC results also show that there is very little change in misfit when an isotopic top layer of is added, as can be seen in Figure 10(b). The error bounds when SC is used are broader than those calculated for FC. A thicker isotropic layer is favoured for the Tr model than for the other three models; the variation in misfit is dominated by ${}_3S_2$ for the Tr model when SC is used, and this mode strongly favours a 400km isotropic layer. Previous normal mode studies may have been unable to satisfy splitting function or spectral data with a model which includes an isotropic layer due to their use of SC. Full-coupling is essential to investigate the possible existence of an isotropic layer at the top of the inner core.

6. Discussion and conclusions

An isotropic top layer at the top of the inner core changes the frequency and attenuation of normal modes. These changes are dependent on the inner core anisotropy model used and on the thickness of the layer. The presence of an isotropic top layer causes an observable effect on synthetic spectra. The magnitude of this effect is of the order of the differences between synthetic and observed seismograms.

The use of full-coupling allows modes such as ${}_{11}S_5$ to respond to changes in isotropic layer thickness at depths greater than would be expected from their sensitivity kernels. The misfit between data and observations is smaller when FC is used than when SC is used, despite the use of SC when the inner core anisotropy models were produced. When FC is used, radial modes respond very strongly to the imposition of an isotropic layer at the top of the inner core; both PKIKP and PKJKP modes are also sensitive to such a structure. PKJKP modes are the only tool which can currently be used to observe shear wave anisotropy in the inner core. The PKJKP modes used here all support an isotropic layer at the top of an anisotropic inner core; and provide the first observation of S-wave isotropy at the top of the inner core.

An isotropic layer of up to 250km thickness at the top of the inner core is compatible with normal mode data. Normal mode observations can therefore be reconciled with the conclusions drawn from body wave studies using the PKiKP and PKPdf phases which permit an isotropic layer of up to 250km (Shearer & Toy, 1991; Song & Helmberger, 1995; Ouzounis & Creager, 2001; Niu & Wen, 2002; Yu & Wen, 2007; Waszek et al., 2011).

The presence of an isotropic layer at the top of the inner core has implications for our understanding of the mechanism which causes inner core anisotropy. Either the mechanism does not require the 'freezing in', or fixing during solidification at the inner core boundary of the anisotropy texture, or the conditions at the inner core boundary (ICB) have changed over time. If the mechanism cannot require the 'freezing in' of anisotropic texture, then the suggestion of Karato (1993b) must be ruled out, as must that of Bergman (1997), who suggest that anisotropy is introduced to the inner core during the solidification process by the effects of the magnetic field at the ICB, or dendritic growth of the crystals. If the conditions at the inner core boundary have changed over time this has significant implications for the history of the Earth's geodynamo and the thermal history of the core.

Buffett (1997) suggests that the top of the inner core may have a lower viscosity than deeper regions. A low viscosity layer of the order of 100km in thickness may then contain small crystals which are seismically isotropic, whilst at greater depths larger crystals may be able to align, producing seismically observable anisotropic fabric below the uppermost isotropic layer.

Acknowledgements

The research leading to these results has received funding from the European Research Council under the European Community's Seventh Framework Programme (FP7/2007-2013)/ERC grant agreement number 204995. JCEI was also supported by a Research Grant from Trinity College, Cambridge. The authors would like to thank Guy Masters for providing both helpful suggestions

and data from his recent measurements of the frequency and quality factor of modes excited by the 2004 Sumatra earthquake; Steve Squires provided useful discussion. This manuscript was improved by the comments of an anonymous reviewer.

References

Beghein, C. & Trampert, J., 2003. Robust normal mode constraints on inner-core anisotropy from model space search, *Science*, **299**, 552–555.

Bergman, M. I., 1997. Measurements of elastic anisotropy due to solidification texturing and the implications for the Earth's inner core, *Nature*, **389**, 60–63.

Buffett, B. A., 1997. Geodynamic estimates of the viscosity of the Earth's inner core, *Nature*, **388**, 571–573.

Cao, A. & Romanowicz, B., 2007. Test of the innermost inner core models using broadband PKIKP travel time residuals, *Geophys. Res. Lett.*, **34**, 8303.

Cao, A. & Romanowicz, B., 2009. Constraints on shear wave attenuation in the Earth's inner core from an observation of PKJKP, *Geophys. Res. Lett.*, **36**, 9301.

Cao, A., Romanowicz, B., & Takeuchi, N., 2005. An observation of PKJKP: Inferences on inner core shear properties, *Science*, **308**, 1453 – 1455.

Cormier, V. F. & Stroujkova, A., 2005. Waveform search for the innermost inner core, *Earth and Planetary Science Letters*, **236**(1-2), 96–105.

Creager, K. C., 1992. Anisotropy of the inner core from differential travel times of the phases PKP and PKIKP, *Nature*, **356**, 309–314.

Creager, K. C., 1999. Large-scale variations in inner core anisotropy, *J. Geophys. Res.*, **104**, 23127–23140.

Creager, K. C., 2000. Inner core anisotropy and rotation, in *Earth's Deep Interior: Mineral Physics and Seismic Tomography from the Atomic to the Global Scale*, edited by S.-I. Karato, L. Stixrude, R. Lieberman, G. Masters, & A. Forte, vol. 117 of **Geophysical Monograph Series**, pp. 89–114, American Geophysical Union.

Dahlen, F. A., 1969. The normal modes of a rotating, elliptical Earth - II. Near-resonance multiplet coupling., *Geophys. J. R. Astron. Soc.*, **18**, 397–436.

Deuss, A., 2008. Normal mode constraints on shear and compressional wave velocity of the Earth's inner core, *Earth and Planetary Science Letters*, **268**, 364–375.

Deuss, A. & Woodhouse, J. H., 2001. Theoretical free-oscillations spectra: the importance of wide band coupling, *Geophys. J. Int.*, **103**, 833–842.

Deuss, A., Woodhouse, J. H., Paulssen, H., & Trampert, J., 2000. The observation of inner core shear waves, *Geophys. J. Int.*, **142**, 67–73.

Dratler, J., Farrell, W. E., Block, B., & Gilbert, F., 1971. High-Q Overtone Modes of the Earth, *Geophys. J. R. Astron. Soc.*, **23**, 399–410.

Durek, J. J. & Ekström, G., 1995. Evidence of bulk attenuation in the asthenosphere from recordings of the Bolivia earthquake, *Geophys. Res. Lett.*, **22**, 2309–2312.

Durek, J. J. & Romanowicz, B., 1999. Inner core anisotropy inferred by direct inversion of normal mode spectra, *Geophys. J. Int.*, **139**, 599–622.

Dziewonski, A. M. & Anderson, D., 1981. Preliminary Reference Earth Model, *Phys. Earth Planet. Inter.*, **25**, 297–356.

Dziewonski, A. M. & Gilbert, F., 1971. Solidity of the inner core of the Earth inferred from normal mode observations, *Nature*, **234**, 465–466.

Garcia, R. & Souriau, A., 2000. Inner core anisotropy and heterogeneity level, *Geophys. Res. Lett.*, **27**(19), 3121–3124.

He, X. & Tromp, J., 1996. Normal-mode constraints on the structure of the mantle and core, *J. Geophys. Res.*, **101**, 20,053–20,082.

Irving, J. C. E., Deuss, A., & Andrews, J., 2008. Wide-band coupling of Earth's normal modes due to anisotropic inner core structure, *Geophys. J. Int.*, **174**.

Ishii, M. & Dziewonski, A. M., 2002. The innermost inner core of the Earth: Evidence for a change in anisotropic behavior at the radius of about 300 km, *Proc. Natl. Acad. Sci. USA*, **99**(22), 14026–14060.

Isse, T. & Nakanishi, I., 2002. Inner-core anisotropy beneath Australia and differential rotation, *Geophys. J. Int.*, **151**(1), 255–263.

Jacobs, J. A., 1953. The Earth's Inner Core, *Nature*, **172**, 297–298.

Karato, S. I., 1993. Importance of anelasticity in the interpretation of seismic tomography, *Geophys. Res. Lett.*, **20**, 1623–1626.

Karato, S. I., 1993. Inner core anisotropy due to the magnetic field-induced preferred orientation of iron, *Science*, **262**, 1708–1711.

Li, X. D., Giardini, D., & Woodhouse, J. H., 1991. The relative amplitudes of mantle heterogeneity in P-velocity, S-velocity and density from free oscillation data, *Geophys. J. Int.*, **105**, 649–657.

Luh, P. C., 1974. Normal Modes of a Rotating, Self-gravitating Inhomogeneous Earth, *Geophys. J. R. Astron. Soc.*, **38**, 187–224.

Masters, G., 2009. Pers. comm.

Masters, G. & Gilbert, F., 1983. Attenuation in the Earth at low frequencies, *Philosophical Transactions of the Royal Society of London. Series A, Mathematical and Physical Sciences*, **308**(1504), 479–522.

Morelli, A., Dziewonski, A. M., & Woodhouse, J. H., 1986. Anisotropy of the inner core inferred from PKIKP travel times, *Geophys. Res. Lett.*, **13**, 1545–1548.

Niu, F. & Wen, L., 2002. Seismic anisotropy in the top 400km of the inner core beneath the "eastern" hemisphere, *Geophys. Res. Lett.*, **29**(12).

Oreshin, S. I. & Vinnik, L. P., 2004. Heterogeneity and anisotropy of seismic attenuation in the inner core, *Geophys. Res. Lett.*, **31**.

Ouzounis, A. & Creager, K. C., 2001. Isotropy overlying anisotropy at the top of the inner core, *Geophys. Res. Lett.*, **28**(22), 4331–4334.

Park, J., 1986. Synthetic seismograms from coupled free oscillations: effects of lateral structure and rotation, *J. Geophys. Res.*, **91**, 6441–6464.

Park, J., Song, T.-R. A., Tromp, J., Okal, E., Stein, S., Roult, G., Clevede, E., Laske, G., Kanamori, H., Davis, P., Berger, J., Braitenberg, C., Van Camp, M., Lei, X., Sun, H., Xu, H., & Rosat, S., 2005. Earth's Free Oscillations Excited by the 26 December 2004 Sumatra-Andaman Earthquake, *Science*, **308**, 1139–1144.

Resovsky, J. S. & Ritzwoller, M. H., 1995. Constraining odd-degree Earth structure with coupled free-oscillations, *Geophys. Res. Lett.*, **22**(16), 2301–2304.

Ritsema, J., van Heijst, H., & Woodhouse, J. H., 1999. Complex shear wave velocity structure imaged beneath Africa and Iceland, *Science*, **286**, 1925–1928.

Rost, S. & Garnero, E. J., 2004. A study of the uppermost inner core from PKKP and P′P′ differential traveltimes, *Geophys. J. Int.*, **1556**, 565–574.

Shearer, P., 1994. Constraints on inner core anisotropy from PKP(df) travel times, *J. Geophys. Res.*, **99**(B10), 19647–19659.

Shearer, P. M. & Toy, K. M., 1991. PKP(BC) versus PKP(DF) differential travel times and aspherical structure in the Earth's inner core, *J. Geophys. Res.*, **96**, 2233–2247.

Song, X. & Helmberger, D. V., 1995. Depth dependence of anisotropy of Earth's inner core, *J. Geophys. Res.*, **100**(B6), 9805–9816.

Song, X. & Helmberger, D. V., 1998. Seismic evidence for an inner core transition zone, *Science*, **282**(5390), 924–927.

Sun, X. & Song, X., 2008. Tomographic inversion for three-dimensional anisotropy of Earth's inner core, *Phys. Earth Planet. Inter.*, **167**, 53–70.

Tanaka, S. & Hamaguchi, H., 1997. Degree one heterogeneity and hemispherical variation of anisotropy in the inner core from PKP(BC)-PKP(DF) times, *J. Geophys. Res.*, **102**(B2), 2925–2938.

Tromp, J., 1993. Support for anisotropy of the Earth's inner core from free oscillation data, *Nature*, **366**, 678–681.

Tsai, V. C., Nettles, M., Ekström, G., & Dziewonski, A. M., 2005. Multiple CMT source analysis of the 2004 Sumatra earthquake, *Geophys. Res. Lett.*, **32**, 17304.

Waszek, L., Irving, J. C. E. & Deuss, A., 2011. Reconciling the hemispherical structure of Earth's inner core with its super-rotation, *Nat. Geosci.*, In press

Woodhouse, J. H., Giardini, D., & Li, X.-D., 1986. Evidence for inner core anisotropy from free oscillations, *Geophys. Res. Lett.*, **13**, 1549–1552.

Wookey, J. & Helffrich, G., 2008. Inner-core shear-wave anisotropy and texture from an observation of PKJKP waves, *Nature*, **454**, 873–876.

Yu, W. & Wen, L., 2007. Complex seismic anisotropy in the top of the Earth's inner core beneath Africa, *J. Geophys. Res.*, **112**(11), 8304.

List of Figures

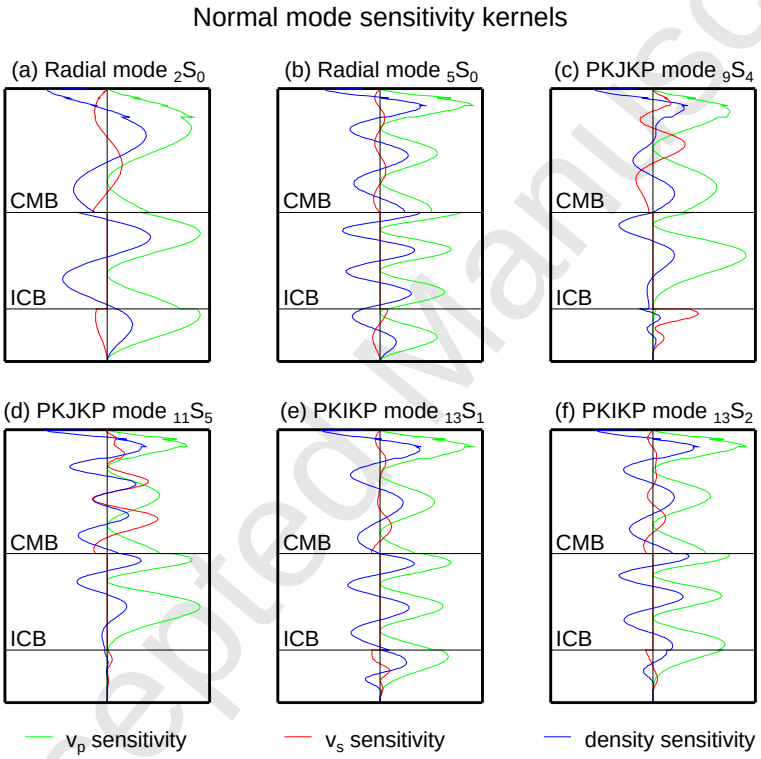

Figure 1: Sensitivity kernels of six inner core sensitive modes: (a)$_2S_0$, (b)$_5S_0$, (c)$_9S_4$, (d)$_{11}S_5$, (e)$_{13}S_1$ and (f)$_{13}S_2$. Sensitivity to v_p is shown in green, v_s is shown in red and density is shown in blue. The locations of the inner core boundary (ICB)and core-mantle boundary (CMB) are also shown.

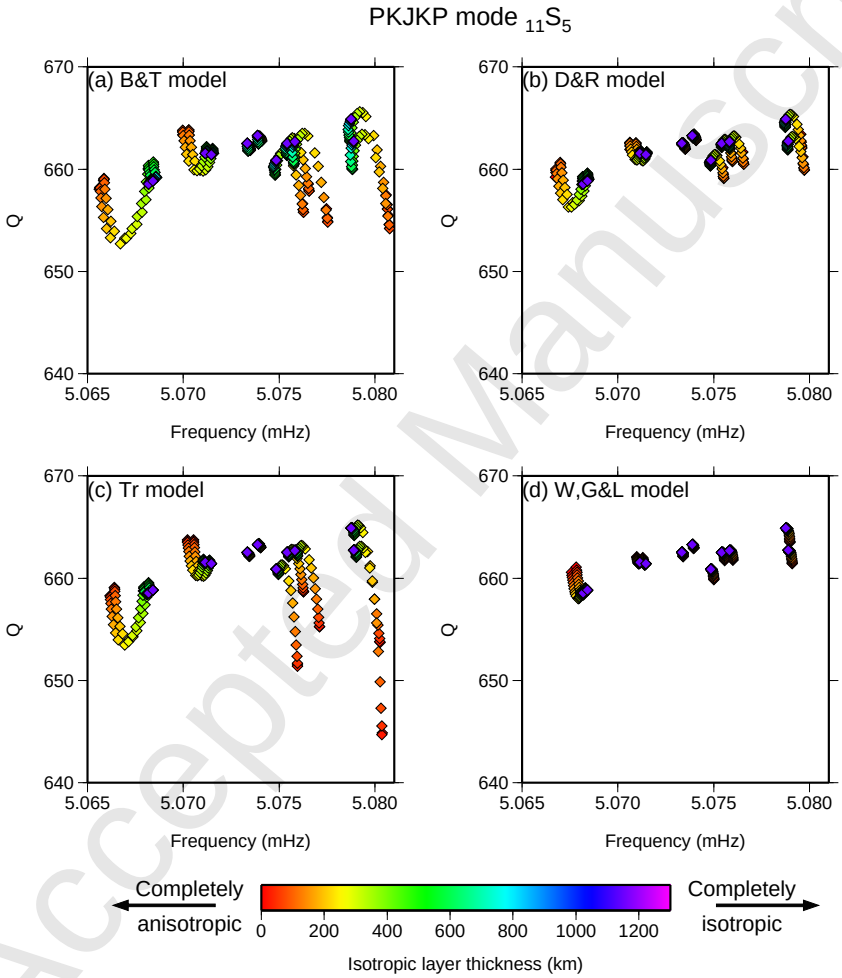

Figure 2: Response of mode $_{11}S_5$ to the inclusion of an isotropic top layer when FC is used.

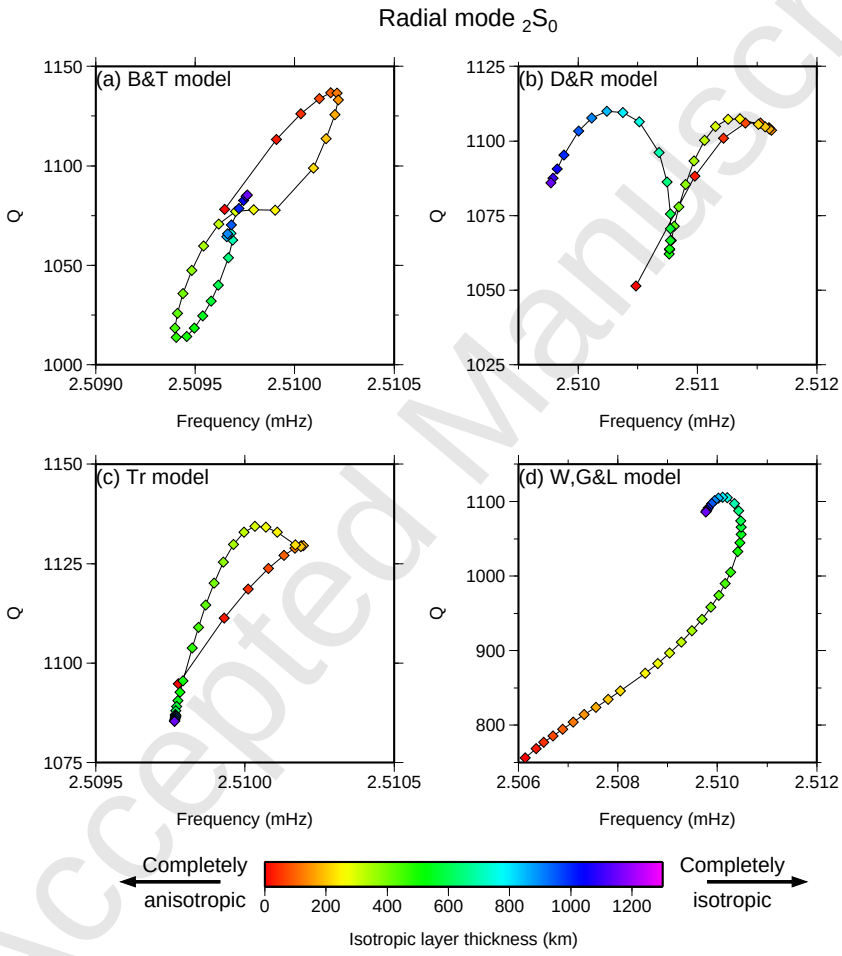

Figure 3: Response of mode $_2S_0$ to the inclusion of an isotropic top layer when FC is used.

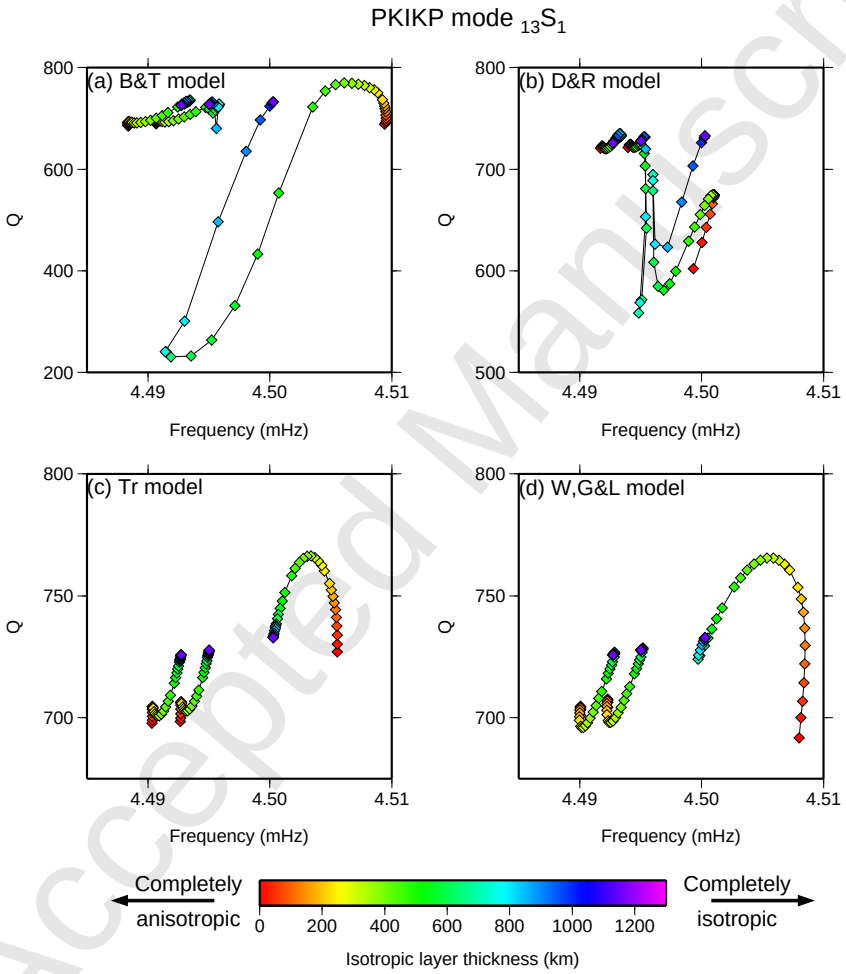

Figure 4: Response of mode $_{13}S_1$ to the inclusion of an isotropic top layer when FC is used.

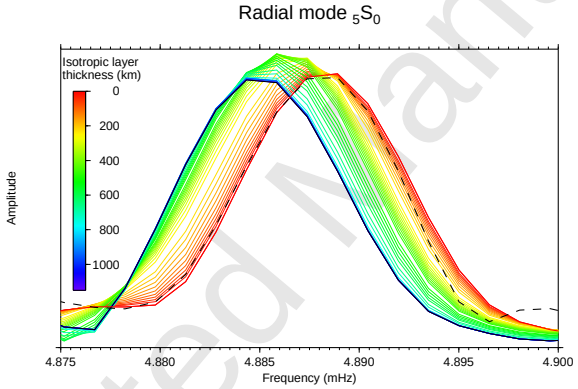

Figure 5: Synthetic spectra for event 122604A, at station ARU, 50-110 hours, for mode $_5S_0$ calculated using full-coupling and B&T anisotropy model. Radial mode $_5S_0$ responds to the introduction of an isotropic top layer on the FC B&T model by decreasing its frequency. Data is shown as a dashed line, and the amplitude of the data has been divided by two for ease of comparison with the synthetic data.

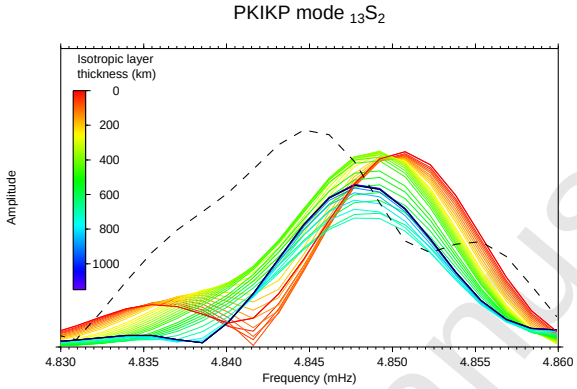

Figure 6: Synthetic spectra for event 122604A, at station ARU, 30-85 hours, for mode $_{13}S_2$ calculated using full-coupling and W,G&L anisotropy model. When there is no isotropic layer, PKIKP mode $_{13}S_2$ is a widely split mode. When an isotropic layer is introduced, the lowest frequency singlets decrease in amplitude and increase in frequencies; the two split spectral peaks merge into one peak as the isotropic layer increases in thickness. Data is shown as a dashed line.

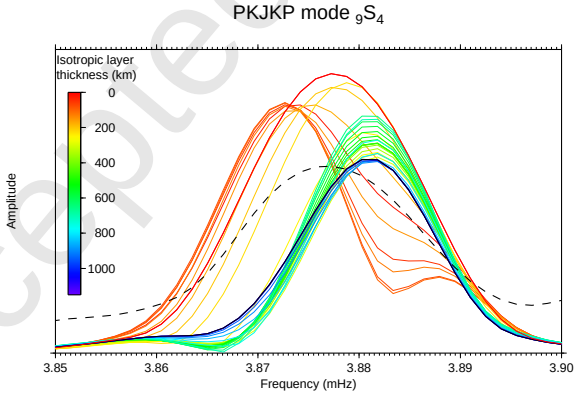

Figure 7: Synthetic spectra for event 060994A, at station ENH, 25-65 hours, for mode $_9S_4$ calculated using full-coupling and D&R anisotropy model. When there is no isotropic layer (red line), PKJKP mode $_9S_4$ is a wide peak. When an isotropic layer is introduced, the amplitude at intermediate frequencies decreases, the spectrum forms into one peak when the isotropic layer is 175km thick. Data is shown as a dashed line.

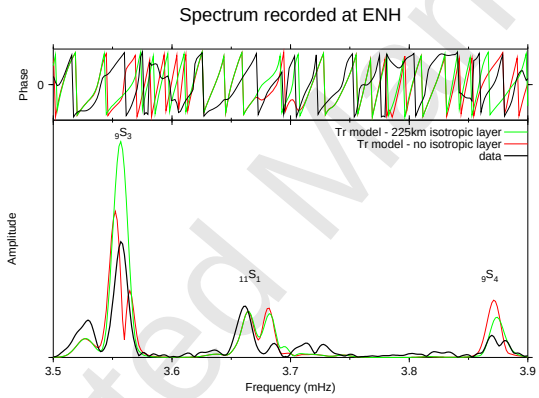

Figure 8: Event 060994A, station ENH, 30-80 hours. Data and synthetic seismograms for the frequency range 3.5-3.9mHz. Three prominent inner core sensitive modes are present in this range: ${}_9S_3$, ${}_{11}S_1$ and ${}_9S_4$. 35 mantle or crust sensitive modes are also present in this frequency window. The two synthetic spectra have been created using FC for the Tr model, with no isotropic layer and a 225km isotropic layer.

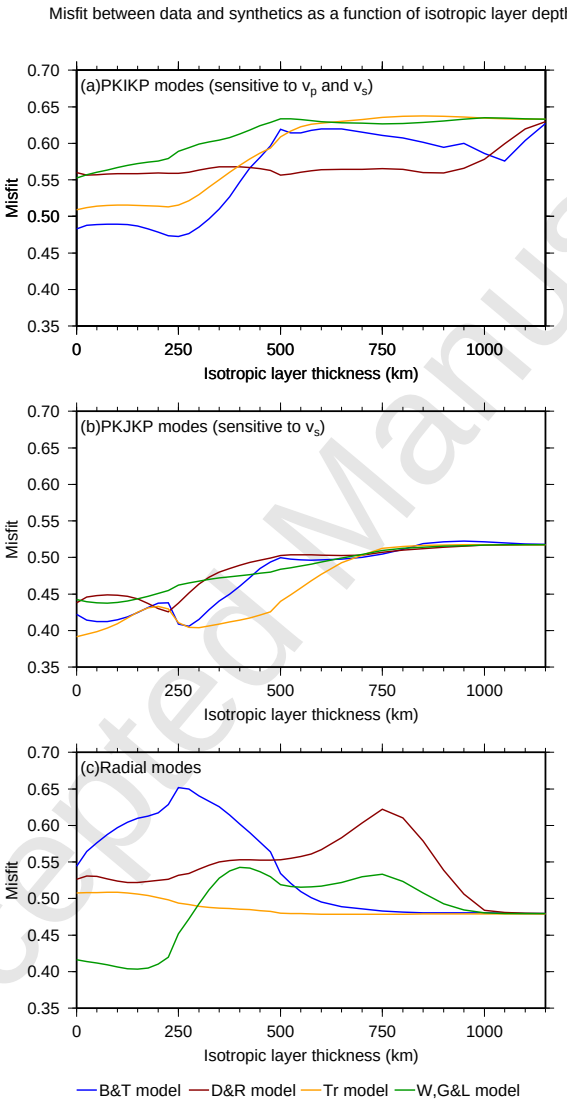

Figure 9: Average misfits between data and FC synthetics seismograms for (a)PKIKP, (b)PKJKP and (c) radial modes when different thicknesses of an isotropic top layer are imposed upon each model.

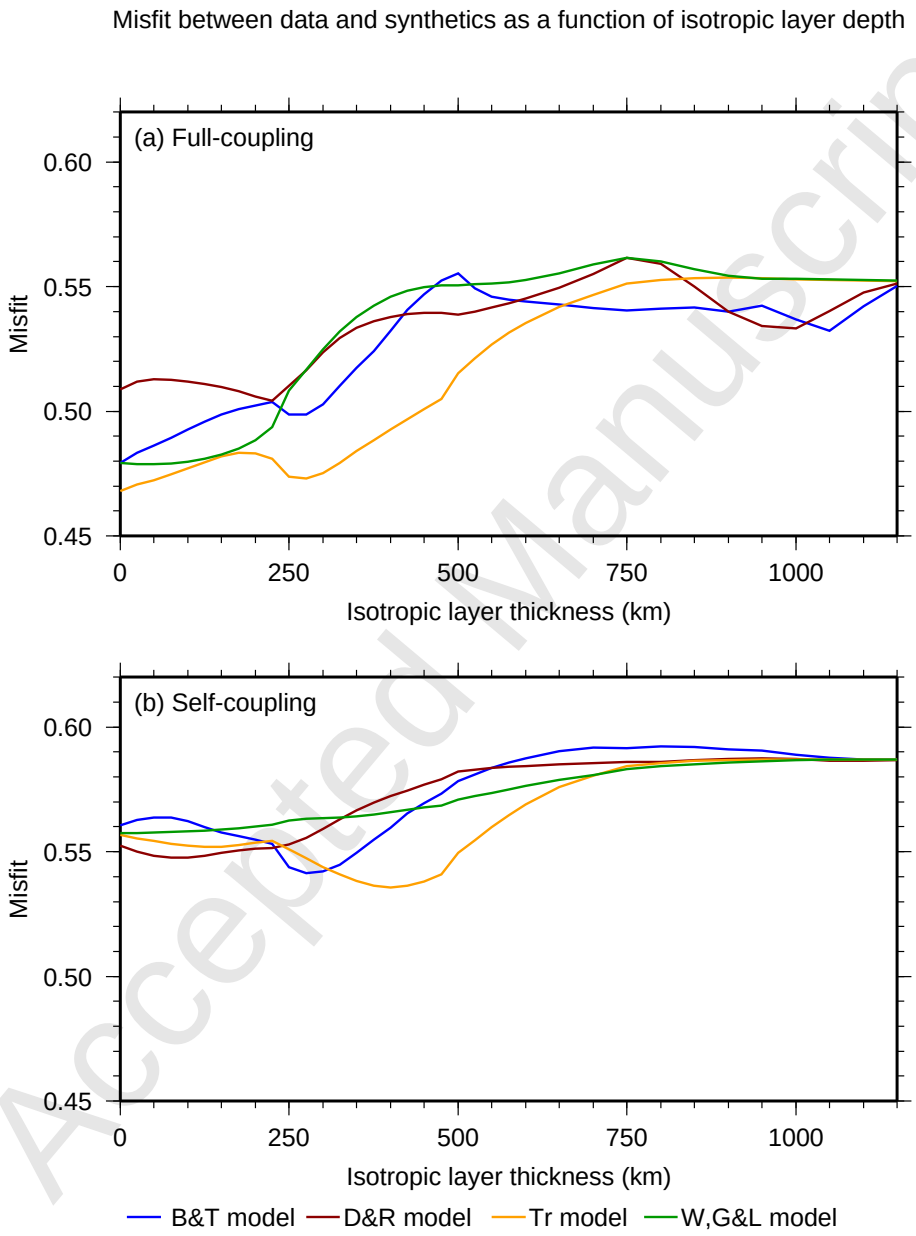

Figure 10: Average misfits between data and synthetics seismograms made using (a) full-coupling and (b) self-coupling for all modes combined when different thicknesses of an isotropic top layer are imposed upon each model.

List of Tables

Table 1: Frequency ranges of normal modes coupled together. The frequency quoted for each mode is that found using PREM with SC, with no inner core or mantle structure included and no ellipticity, rotation corrections. As a 1-D velocity model is used, all of the singlets in each mode oscillate at exactly the same frequency. Each mode is characterised as a radial, PKIKP or PKJKP mode.

Target mode	Mode frequency (mHz)	Frequency range of mantle and crust sensitive modes coupled with target mode (mHz)	Mode character	Number of spectra
${}_3S_2$	1.106	0.000 – 3.000	PKJKP	89
${}_1S_0$	1.631	0.000 – 3.000	Radial	104
${}_6S_1$	1.980	0.000 – 3.000	PKJKP	104
${}_2S_0$	2.510	1.833 – 3.000	Radial	111
${}_6S_3$	2.822	2.380 – 3.397	PKJKP	174
${}_8S_1$	2.873	2.380 – 3.397	PKIKP	166
${}_3S_0$	3.270	2.600 – 3.700	Radial	95
${}_9S_3$	3.555	3.230 – 4.150	PKJKP	112
${}_{11}S_1$	3.685	3.230 – 4.150	PKIKP	95
${}_9S_4$	3.878	3.230 – 4.150	PKJKP	104
${}_{10}S_2 - {}_{11}S_2$	4.032 – 4.059	3.750 – 4.436	PKIKP	151
${}_4S_0$	4.106	3.750 – 4.436	Radial	111
${}_8S_5$	4.166	3.750 – 4.436	PKIKP	111
${}_{13}S_1$	4.499	4.200 – 4.470	PKIKP	118
${}_{11}S_4$	4.767	4.470 – 5.050	PKJKP	107
${}_{13}S_2$	4.845	4.470 – 5.050	PKIKP	98
${}_5S_0$	4.884	4.470 – 5.050	Radial	88
${}_{11}S_5$	5.074	4.820 – 5.360	PKJKP	177
${}_{13}S_3$	5.194	4.960 – 5.429	PKIKP	136

Table 2: Details of the four events used. Information is taken from the global CMT catalogue (`www.globalcmt.org`).

CMT Code	Date	Time (GMT)	Lat. (°N)	Lon. (°E)	depth (km)	Half-duration (s)	M_w
060994A	1994/06/09	00:33:45.4	-13.82	-67.25	647.1	20.0	8.2
100494B	1994/10/04	13:23:28.5	43.60	147.63	68.2	25.0	8.3
073095A	1995/07/30	05:11:56.9	-24.17	-70.74	28.7	16.0	8.0
122604A	2004/12/26	01:01:09.0	3.09	94.26	28.6	95.0	9.0

Table 3: Frequency and Q measurements for mode ${}_2S_0$. Measurements from Masters (2009) were made on data collected from the Sumatra event and have been calculated independently of this study.

Reference	Frequency (mHz)	Q
PREM prediction (Dziewonski & Anderson, 1981)	2.5105	1241.6
He & Tromp (1996)	2.50977 ± 0.00002	1721 ± 183
Masters & Gilbert (1983)	2.5079 ± 0.00025	1802 ± 450
Dratler et al. (1971)	2.5082	–
Dziewonski & Gilbert (1971)	2.5092	–
Masters (2009)	2.50797 ± 0.00002	1208 ± 8

Table 4: Frequency and Q measurements for mode ${}_5S_0$. Measurements from Masters (2009) were made on data collected from the Sumatra event and have been calculated independently of this study

Reference	Frequency (mHz)	Q
PREM prediction (Dziewonski & Anderson, 1981)	4.8842	920.8
He & Tromp (1996)	4.88848 ± 0.00002	1181 ± 78
Masters & Gilbert (1983)	4.8891 ± 0.0001	1250 ± 120
Dratler et al. (1971)	4.8873	–
Durek & Ekström (1995)	–	1096 ± 50
Masters (2009)	4.88827 ± 0.00002	1068 ± 2

Table 5: Best fitting isotropic top layer thickness, for all modes. The error bounds are defined as being thicknesses for which the misfit is within 0.005 of its minimum value. The secondary minima are also shown for the FC synthetic seismograms.

Model	Preferred isotropic layer thickness (km), and error bounds		
	FC		SC
	Primary minima	Secondary minima	Minima
B&T	0 (0-25)	275	275 (250-325)
D&R	225 (175-225)	0	75 (0-225)
Tr	0 (0-50)	275	400 (350-450)
W,G&L	25 (0-150)	-	25 (0-225)